HHS Public Access

Author manuscript

J Mater Res. Author manuscript; available in PMC 2016 May 27.

Published in final edited form as:

J Mater Res. 2016 February 15; 31(3): 321–327. doi:10.1557/jmr.2015.406.

Repair of dentin defects from DSPP knockout mice by PILP mineralization

H. Nurrohman,
Department of Preventive and Restorative Dental Sciences, University of California, San Francisco, San Francisco, California 94143, USA

K. Saeki,
Department of Preventive and Restorative Dental Sciences, University of California, San Francisco, San Francisco, California 94143, USA

K. Carneiro,
Department of Preventive and Restorative Dental Sciences, University of California, San Francisco, San Francisco, California 94143, USA

Y.C. Chien,
Department of Preventive and Restorative Dental Sciences, University of California, San Francisco, San Francisco, California 94143, USA

S. Djomehri,
Department of Preventive and Restorative Dental Sciences, University of California, San Francisco, San Francisco, California 94143, USA

S.P. Ho,
Department of Preventive and Restorative Dental Sciences, University of California, San Francisco, San Francisco, California 94143, USA

C. Qin,
Department of Biomedical Sciences and Center for Craniofacial Research and Diagnosis, Texas A&M University Baylor College of Dentistry, Dallas, Texas 75246, USA

S.J. Marshall,
Department of Preventive and Restorative Dental Sciences, University of California, San Francisco, San Francisco, California 94143, USA

L.B. Gower,
Department of Materials Science & Engineering, University of Florida, Gainesville, Florida 32611, USA

G.W. Marshall, and
Department of Preventive and Restorative Dental Sciences, University of California, San Francisco, San Francisco, California 94143, USA

S. Habelitz[a)]

[a)]Address all correspondence to this author. ; Email: Stefan.Habelitz@ucsf.edu

The authors declare no potential conflicts of interest with respect to the authorship and/or publication of this article.

Department of Preventive and Restorative Dental Sciences, University of California, San Francisco, San Francisco, California 94143, USA

Abstract

Dentinogenesis imperfecta type II (DGI-II) lacks intrafibrillar mineral with severe compromise of dentin mechanical properties. A *Dspp* knockout ($Dspp^{-/-}$) mouse, with a phenotype similar to that of human DGI-II, was used to determine if poly-L-aspartic acid [poly(ASP)] in the "polymer-induced liquid-precursor" (PILP) system can restore its mechanical properties. Dentin from six-week old $Dspp^{-/-}$ and wild-type mice was treated with CaP solution containing poly(ASP) for up to 14 days. Elastic modulus and hardness before and after treatment were correlated with mineralization from Micro x-ray computed tomography (Micro-XCT). Transmission electron microscopy (TEM)/Selected area electron diffraction (SAED) were used to compare matrix mineralization and crystallography. Mechanical properties of the $Dspp^{-/-}$ dentin were significantly less than wild-type dentin and recovered significantly ($P < 0.05$) after PILP-treatment, reaching values comparable to wild-type dentin. Micro-XCT showed mineral recovery similar to wild-type dentin after PILP-treatment. TEM/SAED showed repair of patchy mineralization and complete mineralization of defective dentin. This approach may lead to new strategies for hard tissue repair.

I. Introduction

Most naturally mineralizing load-bearing tissues, such as bone and dentin, are composed of type I collagen fibrils and noncollagenous proteins (NCPs) that form a scaffold reinforced with intrafibrillar and extrafibrillar minerals.[1,2] The two hydrolysis products of the dentin sialophosphoprotein (DSPP), the dentin sialoprotein (DSP) and dentin phosphoprotein (DPP), have been shown to be critical for proper dentin biomineralization that is attributed to their highly anionic and calcium binding properties.[3,4]

Human genetic studies have demonstrated that mutations in the *DSPP* gene result in dentinogenesis imperfecta type II (DGI-II),[5,6] characterized by dentin hypomineralization and lack of intrafibrillar mineral with severe compromise of the mechanical properties of dentin.[1,2] Most interestingly, animal studies revealed that *Dspp* knockout ($Dspp^{-/-}$) mice have dentin defects that closely resemble human DGI-II.[7] These mice may serve as a model for human DGI-II and would provide a unique opportunity for the study of the importance of NCPs on mineral-collagen interaction and biomechanical response. Inspired by the properties of biomineralization-related NCPs, Gower and coworkers achieved intrafibrillar mineralization of a variety of collagen substrates using poly-L-aspartic acid [poly(ASP)], in the so-called "polymer-induced liquid-precursor" (PILP) system.[8,9] Similar biomimetic approaches using other polyanionic acids have been reported by Tay and Pashley and Nudelman et al.[10,11] The use of a simple synthetic polymer as an analog for NCPs is critical for understanding the basic principles of mineral–collagen interactions.[12]

We therefore studied the possibility of mineralization of collagen in the DGI-II mouse model and tested the hypothesis that poly(ASP), as used for PILP mineralization, may restore the mechanical properties of dentin, a critical role attributed to DSPP protein. Dentin repair and engineering of a DGI-II mouse model were examined by the change in elastic modulus,

hardness, and mineral content. We related these changes to their ultramorphology and crystal distribution.

II. Experimental

A. Sample preparation

Wild-type (*Dspp*$^{+/+}$) and both homozygous (*Dspp*$^{-/-}$), and heterozygous (*Dspp*$^{+/-}$) male mice at 6 wks, 3 of each, were used in this study, provided by Dr. Chunlin Qin (Baylor College of Dentistry, Dallas, TX).

Mandibles were dissected and sterilized using gamma radiation and stored in Hank's balanced salt solution at 4 °C until prepared.[13] The animal protocol and procedures were approved by the committee on animal research at UCSF. The dissected mandibles were embedded in epoxy resin (Epoxicure, Buehler, Lake Bluff, IL). The mesial surface of a mandibular first molar was then cross-sectioned in the buccolingual direction to expose the occlusal surface inwards toward the dentin-enamel junction (DEJ) and pulp chamber. Specimens were cross-sectioned and sagittal surfaces were polished with SiC-papers and aqueous diamond suspensions to 0.25 μm.

B. Mineralization Experiments

Each cross-sectioned surface in *Dspp*$^{-/-}$ specimens was immersed in 40 mL of PILP mineralization system (n = 3) and incubated at 37 °C under continuous stirring for 14 days. The mineralization solution was prepared following a previously reported protocol.[14] Poly(ASP) (MW: 27 KDa; Alamanda Polymers, Huntsville, AL) was used and added to a Tris-buffered calcium chloride dihydrate solution at pH 7.4 containing sodium azide (0.02%). An equal volume of dipotassium phosphate solution was added, resulting in final concentrations of 4.5 mM Ca^{2+}, 2.1 mM PO_4^{3-}, and 100 μg/mL poly(ASP). In this study, cross-sectioned surfaces in wild-type specimens were used as a control (n = 3).

C. Nanoindentation

The cross-sectioned specimens were fixed to a atomic force microscope (AFM) metal specimen discs using a very thin layer of cyanoacrylate adhesive (MDS Products, Inc., Laguna Hills, CA). Wet nanoindentation was performed in a liquid cell filled with deionized water using an AFM (Nanoscope III Veeco Instruments, Santa Barbara, CA) to which a load-displacement transducer (Triboscope, Hysitron Inc., Minneapolis, MN) was attached. The *Dspp*$^{-/-}$ specimens were tested before and after PILP treatment (n = 3) and compared to wild-type specimens (n = 3). A sharp diamond Berkovich indenter with a conventional radius of curvature less than 100 nm was fitted to the transducer. Fused silica was used to calibrate the transducer under dry and wet conditions. Site-specific measurements of reduced elastic modulus (E_r) and hardness (H) were made using a controlled force of 300 μN with a 3-s trapezoidal loading profile (load, hold, and unload) as is our standard practice.[2,15,16] Indentations were made at intervals of 4 μm starting in mid-coronal dentin or at the DEJ and continuing over 200 μm into dentin. Two similar lines of indents were made in each specimen. The data were statistically analyzed by one-way ANOVA and Tukey's multiple comparison tests with statistical significance were set at $\alpha = 0.05$.

D. Micro x-ray computed tomography (Micro-XCT)

Following mechanical characterization, a representative specimen from each group of the *Dspp*$^{-/-}$ mice was scanned before and after PILP-treatment using Micro-XCT (Xradia MicroXCT-200, Carl Zeiss X-ray Micros-copy, Inc., Pleasanton, CA) following protocols described previously.[14,17] Scanning parameters used were 10× magnification, a peak voltage of 50 kVp, 133 μA, and 2000 image projections, with a pixel size of 1.67 μm. Intensity resulting from x-ray attenuation due to mineral density variation within experimental region was compared with wild-type dentin using XMController version 8.2.3724, the data acquisition software for the Micro-XCT, by selecting line profiles from the mid-coronal dentin surface toward the pulp. To detect the depth of mineralization, intensity of virtual slices of *Dspp*$^{-/-}$ dentin before and after PILP-treatments with regions of interest (ROI) from the surface into subsurface layers were plotted and compared. Tomograms of *Dspp*$^{-/-}$ mice after PILP-treatment were subsequently postprocessed to segment out volumes with different mineral densities with Avizo Fire 8.1 software (Visage Imaging Inc., San Diego, CA) using the 3D digital segmentation method previously described by Djomehri et al.[17]

E. Transmission electron microscopy (TEM)

The dissected mandibles were embedded in epoxy resin and first molar specimens from the *Dspp*$^{-/-}$ mice before and after PILP-treatments (n = 3) were prepared and processed for TEM according to a previously reported protocol.[14] Briefly, specimens were further trimmed and embedded in ethyl alcohol followed by acetone dehydration in Spurr's resin (Ted Pella, Redding, CA). Unstained, 70–80 nm thick sections were examined by means of a FEI Tecnai T12 TEM (FEI, Hillsboro, OR) at 120 kV. Selected area electron diffraction (SAED) patterns were performed using an aperture that selected a 200 nm diameter area of the TEM section; the *d*-spacings of the diffraction pattern were calibrated using the *d*-spacings of gold determined under identical conditions.[18] SAED provided corroborative evidence for the presence of apatite crystallites before and after PILP mineralization.

III. Results

A. Nanoindentation

When evaluating nanomechanical properties of dentin from 6-wk-old mice, we found no significant differences between wild-type (*Dspp*$^{+/+}$) and *Dspp*$^{+/-}$ (heterozygous) dentin specimens. The *Dspp*$^{-/-}$ dentin (homozygous), however, was significantly lower in elastic modulus (E_r) and hardness (H) with average values of about 5.4 ± 1.6 and 0.17 ± 0.07 GPa, respectively. The nanomechanical properties of the *Dspp*$^{-/-}$ dentin was about 1/3 of the value measured for wild-type's dentin (E_r = 14.3 ± 0.9, H = 0.4 ± 0.1) when comparing lines of indentations from the mid-coronal dentin to the pulp (Fig. 1).

Interestingly, the nanomechanical properties recovered substantially with the PILP mineralization treatment after 14 days of treatment ($P < 0.05$). The average of all data points showed that E_r (11.03 ± 0.9) and H (0.35 ± 0.02) of *Dspp*$^{-/-}$ dentin more than doubled after PILP and reached 77 and 82% of the normal value of wild-type (control), respectively (Fig. 1).

B. Micro-XCT

Typical Micro-XCT images are shown for the *Dspp*$^{-/-}$ group before and after PILP-treatment, and the wild-type mice (Fig. 2(A)). Before PILP-treatment, *Dspp*$^{-/-}$ mice showed defective dentin (patchiness) with irregular shapes. Interestingly, following PILP-treatment, the mineralized specimens revealed more uniform mineralization with decreased patchiness, so that the appearance was comparable with the wild-type specimen.

Figure 2(B) shows the intensity profiles along a line across a sagittal section of *Dspp*$^{-/-}$ dentin before and after PILP-treatment. The line plot revealed a marked increase in x-ray attenuation following PILP-treatment with levels approaching wild-type control. A plot of ROIs from the outer surface inward from *Dspp*$^{-/-}$ dentin before and after PILP-treatment revealed only a few micrometers of depth [Fig. 2(C)]. 3D image segmentation of *Dspp*$^{-/-}$ mice visualized that PILP-treatment created a few micrometers of an interaction layer formed of apatite crystals on the dentin surface [Fig. 2(D)].

C. Transmission electron microscopy

Representative TEM images of the *Dspp*$^{-/-}$ mice group before and after PILP-treatment are shown in Fig. 3. It should be noted that the TEM samples were not stained with any electron-dense substance. Before PILP-treatment, the electron-dense apatite mineral of the intertubular dentin was sparsely and heterogeneously distributed within the body of the collagen scaffold matrix [Figs. 3(A) and 3(B)]. This region generated separate diffraction arcs along the (002) plane *d*-spacing of apatite (Fig. 3(B)-inset), indicating that the crystallites had the preferred orientation of low-density (high porosity) apatite crystals.[19] After PILP-treatment, the collagenous matrix showed uniform mineralization characterized by electron-dense intrafibrillar and/or extrafibrillar apatite crystals [Figs. 3(C) and 3(D)]. Banding patterns of collagen fibers were obscured [Fig. 3(D)], indicating that the collagen is heavily mineralized and covers collagen fibrils.[20] In addition, continuous SAED ring patterns ascribed to the major (002) and (211) planes *d*-spacing of apatite [Fig. 3(D)-inset] were exhibited, suggesting a denser overall crystallite arrangement in this treated dentin.

IV. Discussion

This study sought to gain insights into the role of highly charged poly(ASP) polymer leading to mineralization and mechanical recovery of a DGI-II mouse model. In the past few years, studies have shown that the PILP system can reintroduce intrafibrillar apatite mineral into collagenous tissues.[8,9,11] It has been proposed that interaction of the polymer with the incipient mineral results in a negatively charged complex that interacts with a positively charged region at the C-terminus end of the gap zone, thus mediating the infiltration of the amorphous calcium phosphate (ACP) into the fibril.[11] Besides charge interactions between the polymer–mineral complex and the fibril, there is evidence that poly(ASP) acts by inhibiting apatite nucleation in solution and stabilizing the formation of a liquid-like, highly hydrated ACP phase. The polymer-stabilized ACP is thought to infiltrate into the collagen fibrils through capillary action, and transforms into oriented apatite crystals.[8] This interaction between collagen and the polymer is essential for the mineralization process and controls the rate of mineral formation.

In human artificial caries, however, full mechanical recovery of mechanical properties of the tissue was only obtained in a zone that was not fully demineralized and had remnant intrafibrillar mineral.[14,21] Other studies by our group showed that the extrafibrillar mineral is dissolved more rapidly than the intrafibrillar mineral.[15,22] Thus, the potential to restore the functionality of dentin increases toward deeper areas of a lesion as more residual mineral, particularly intrafibrillar mineral, will have survived the acid dissolution process and can grow in size during the remineralization process.[15,16,21] Functional mineralization is the term used to distinguish mechanical property recovery in hydrated samples from simple mineral precipitation between the collagen fibrils, mainly extrafibrillar mineral formation.[23] This type of mineralization could show an increase in mineral content but mechanical recovery is very limited without a tight association of apatite to the collagen matrix. Here we used genetically modified mice lacking the *Dspp* gene. Previous studies showed that the dentin of these mice is thinner, the dental pulp is enlarged,[7] and apatite mineral particles in the dentin are not homogenously distributed, but appear in patches similar to the data of TEM analysis in Fig. 3. Modulus and hardness plots by nanoindentation across dentin showed overall reduced values (E_r = 5.4, H = 0.17) for defective dentin. It should be noted that $Dspp^{-/-}$ dentin had higher standard deviation; reflecting heterogeneity of mineral distribution [Figs. 1(D) and 1(E)]. Moreover, there was substantial variation with lowest modulus values at 2.4 GPa and highest values at 7.6 GPa [Fig. 1(A)], possibly associated with the heterogeneity of mineral distribution. The lower mineral content might be related to a complete absence of intrafibrillar mineral as observed in human DGI-II cases.[1,2] The main support of the dentin tissue derives from extrafibrillar mineral, which appears scattered across the mid-coronal dentin fairly randomly according to our TEM analysis. Others have shown that mineralization of dentin is initiated at the predentin-dentin interface which forms the mineralization front, characterized by the presence of multiple globular mineral foci “calcospherites”. These calcospherites grow and coalesce with the adjacent calcospherites to form a relatively uniform mineralization front. It was suggested that, in the absence of DSPP protein, calcospherites have failed to fuse into a homogenous mass within mature dentin and leave the poorly mineralized patch of collagen matrix.[7] Interestingly, our analysis by Micro-XCT, TEM, and SAED of $Dspp^{-/-}$ dentin revealed patchiness and calcospherites of the mineral crystals of dentin [Figs. 2(A), 3(A), and 3(B)] similar to those of the DGI-II patients[24] and confirm previous findings on the $Dspp^{-/-}$ mice.[25]

In this study, we applied PILP-treatment for 14 days with the intention to repair the mineralization defects of dentin from the $Dspp^{-/-}$ mice and to recover both mineral content and tissue properties to sound tissue values. Our image analyses showed that the patchiness was strongly reduced in Micro-XCT [Fig. 2(A)] with the formation of new apatite crystals named as “Interaction Layer” that penetrated into the dentin [Fig. 2(D)]. Although the repair kinetics and extent of this interaction layer (<10 μm depth) was limited in the current work, the fact that it was achieved is encouraging for further study on remineralization as well as for treatments of dentin hypersensitivity. Other biomimetic remineralization approaches have shown improved rates of mineralization by combining polyacrylic acid and L-glutamic acid for calcium phosphate delivery to demineralized dentin.[26] In this study, mineral distribution was homogenous after PILP-treatment as indicated by a continuous and complete layer of mineral in PILP treated dentin [Figs. 3(C) and 3(D)]. In agreement with the structural

analysis, nanomechanical properties also recovered substantially in the *Dspp*$^{-/-}$ dentin after PILP-treatment (Fig. 1). In some areas modulus and hardness values reached values of normal dentin. When averaged overall data points, modulus and hardness of *Dspp*$^{-/-}$ dentin more than doubled after PILP and reached 77 and 82% of the normal value, respectively. This suggests that PILP-treatments are able to reintroduce mineral into a defective tissue and generate intrafibrillar mineral similar to treatments on collagen fibers or demineralized dentin.

We therefore hypothesize that poly(ASP) acts in vitro in a similar way as DSPP protein in vivo as it was able to restore most of the functions in these mice displaying a DGI-II phenotype. DSPP protein and its hydrolysis products, DSP and DPP, may therefore function as delivery agents, carry calcium and phosphate ions to dentin collagen fibrils and allow for deposition of these ions into the gap-zone in fibrils as demonstrated in vitro for collagen mineralization by poly(ASP). Once calcium and phosphate ions have infused the fibril; mineral solidifies in an amorphous state and gradually transforms into oriented intrafibrillar apatite crystallites. In addition, our results further provide evidence that PILP mineralization system does not rely solely on seed crystallites of remnant intrafibrillar mineral to achieve functional mineralization.

V. Conclusions

In summary, the results presented in this study provide critical insights into the mechanism of poly(ASP)-mediated intrafibrillar mineralization of dentin collagen and suggest the possibility of repairing congenital defects in dentin through biomimetic PILP mineralization system. Optimization of a biomimetic mineralization approach can open new pathways toward an in situ strategy that may develop into clinically-relevant biomedical applications to hard tissue repair and engineering.

Acknowledgments

This work was supported by NIH Grants 2R01 DE016849 and CTSI-SOS Grant Award #000166. Micro-XCT imaging work was performed at the Division of Biomaterials and Bioengineering μCT Imaging Facility, UCSF, supported by S10 Shared Instrumentation Grant (S10RR026645).

References

1. Kinney JH, Pople JA, Driessen CH, Breunig TM, Marshall GW, Marshall SJ. Intrafibrillar mineral may be absent in dentinogenesis imperfecta type II (DI-II). J Dent Res. 2001; 80(6):1555. [PubMed: 11499512]
2. Kinney JH, Habelitz S, Marshall SJ, Marshall GW. The importance of intrafibrillar mineralization of collagen on the mechanical properties of dentin. J Dent Res. 2003; 82(12):957. [PubMed: 14630894]
3. Deshpande AS, Fang PA, Zhang X, Jayaraman T, Sfeir C, Beniash E. Primary structure and phosphorylation of dentin matrix protein 1 (DMP1) and dentin phosphophoryn (DPP) uniquely determine their role in biomineralization. Biomacromolecules. 2011; 12(8):2933. [PubMed: 21736373]
4. Gibson MP, Zhu Q, Liu Q, D'Souza RN, Feng JQ, Qin C. Loss of dentin sialophosphoprotein leads to periodontal diseases in mice. J Periodontal Res. 2013; 48(2):221. [PubMed: 22934831]

5. Kim JW, Nam SH, Jang KT, Lee SH, Kim CC, Hahn SH, Hu JC, Simmer JP. A novel splice acceptor mutation in the DSPP gene causing dentinogenesis imperfecta type II. Hum Genet. 2004; 115(3): 248. [PubMed: 15241678]

6. Kim JW, Hu JC, Lee JI, Moon SK, Kim YJ, Jang KT, Lee SH, Kim CC, Hahn SH, Simmer JP. Mutational hot spot in the DSPP gene causing dentinogenesis imperfecta type II. Hum Genet. 2005; 116(3):186. [PubMed: 15592686]

7. Sreenath T, Thyagarajan T, Hall B, Longenecker G, D'Souza R, Hong S, Wright JT, MacDougall M, Sauk J, Kulkarni AB. Dentin sialophosphoprotein knockout mouse teeth display widened predentin zone and develop defective dentin mineralization similar to human dentinogenesis imperfecta type III. J Biol Chem. 2003; 278(27):24874. [PubMed: 12721295]

8. Olszta MJ, Odom DJ, Douglas EP, Gower LB. A new paradigm for biomineral formation: Mineralization via an amorphous liquid-phase precursor. Connect Tissue Res. 2003; 44(Suppl 1): 326. [PubMed: 12952217]

9. Gower LB. Biomimetic model systems for investigating the amorphous precursor pathway and its role in biomineralization. Chem Rev. 2008; 108(11):4551. [PubMed: 19006398]

10. Tay FR, Pashley DH. Guided tissue remineralisation of partially demineralised human dentine. Biomaterials. 2008; 29(8):1127. [PubMed: 18022228]

11. Nudelman F, Pieterse K, George A, Bomans PH, Friedrich H, Brylka LJ, Hilbers PA, de with G, Sommerdijk NA. The role of collagen in bone apatite formation in the presence of hydroxyapatite nucleation inhibitors. Nat Mater. 2010; 9(12):1004. [PubMed: 20972429]

12. Nurrohman H, Nakashima S, Takagaki T, Sadr A, Nikaido T, Asakawa Y, Uo M, Marshall SJ, Tagami J. Immobilization of phosphate monomers on collagen induces biomimetic mineralization. Bio-med Mater Eng. 2015; 25(1):89.

13. Habelitz S, Marshall GW Jr, Balooch M, Marshall SJ. Nanoindentation and storage of teeth. J Biomech. 2002; 35(7):995. [PubMed: 12052404]

14. Burwell AK, Thula-Mata T, Gower LB, Habelitz S, Kurylo M, Ho SP, Chien YC, Cheng J, Cheng NF, Gansky SA, Marshall SJ, Marshall GW. Functional remineralization of dentin lesions using polymer-induced liquid-precursor process. PLoS One. 2012; 7(6):e38852. [PubMed: 22719965]

15. Habelitz S, Balooch M, Marshall SJ, Balooch G, Marshall GW Jr. In situ atomic force microscopy of partially demineralized human dentin collagen fibrils. J Struct Biol. 2002; 138(3):227. [PubMed: 12217661]

16. Bertassoni LE, Habelitz S, Marshall SJ, Marshall GW. Mechanical recovery of dentin following remineralization in vitro—An indentation study. J Biomech. 2011; 44(1):176. [PubMed: 20926080]

17. Djomehri SI, Candell S, Case T, Browning A, Marshall GW, Yun W, Lau SH, Webb S, Ho SP. Mineral density volume gradients in normal and diseased human tissues. PLoS One. 2015; 10(4):e0121611. [PubMed: 25856386]

18. Nurrohman H, Nikaido T, Takagaki T, Sadr A, Ichinose S, Tagami J. Apatite crystal protection against acid-attack beneath resin-dentin interface with four adhesives: TEM and crystallography evidence. Dent Mater. 2012; 28(7):e89. [PubMed: 22572538]

19. Zavgorodniy AV, Rohanizadeh R, Swain MV. Ultrastructure of dentine carious lesions. Arch Oral Biol. 2008; 53(2):124. [PubMed: 17915189]

20. Thula-Mata T, Burwell A, Gower LB, Habeliz S, Marshall GW. Remineralization of artificial dentin lesions via the polymer-induced liquid-precursor (PILP) process. Mater Res Soc Symp Proc. 2011; 1355:1114. [PubMed: 24839340]

21. Habelitz S, Hsu T, Hsiao P, Saeki K, Chien YC, Marshall SJ, Marshall GW. The natural process of biomineralization and in-vitro remineralization of dentin lesions. 1. Advances in bio-ceramics and biotechnologies II. Ceram Trans. 2014; 247:13.

22. Balooch M, Habelitz S, Kinney JH, Marshall SJ, Marshall GW. Mechanical properties of mineralized collagen fibrils as influenced by demineralization. J Struct Biol. 2008; 162(3):404. [PubMed: 18467127]

23. Bertassoni LE, Habelitz S, Kinney JH, Marshall SJ, Marshall GW Jr. Biomechanical perspective on the remineralization of dentin. Caries Res. 2009; 43(1):70. [PubMed: 19208991]

24. Levin LS, Leaf SH, Jelmini RJ, Rose JJ, Rosenbaum KN. Dentinogenesis imperfecta in the brandywine isolate (DI type III): Clinical, radiologic, and scanning electron microscopic studies of the dentition. Oral Surg Oral Med Oral Pathol. 1983; 56(3):267. [PubMed: 6579461]

25. Fang PA, Verdelis K, Yang X, Lukashova L, Boskey AL, Beniash E. Ultrastructural organization of dentin in mice lacking dentin sialo-phosphoprotein. Connect Tissue Res. 2014; 55(Suppl 1):92. [PubMed: 25158189]

26. Sun J, Chen C, Pan H, Chen Y, Mao C, Wang W, Tang R, Gu X. Biomimetic promotion of dentin remineralization using L-glutamic acid: Inspiration from biomineralization proteins. J Mater Chem B. 2014; 2:4544.

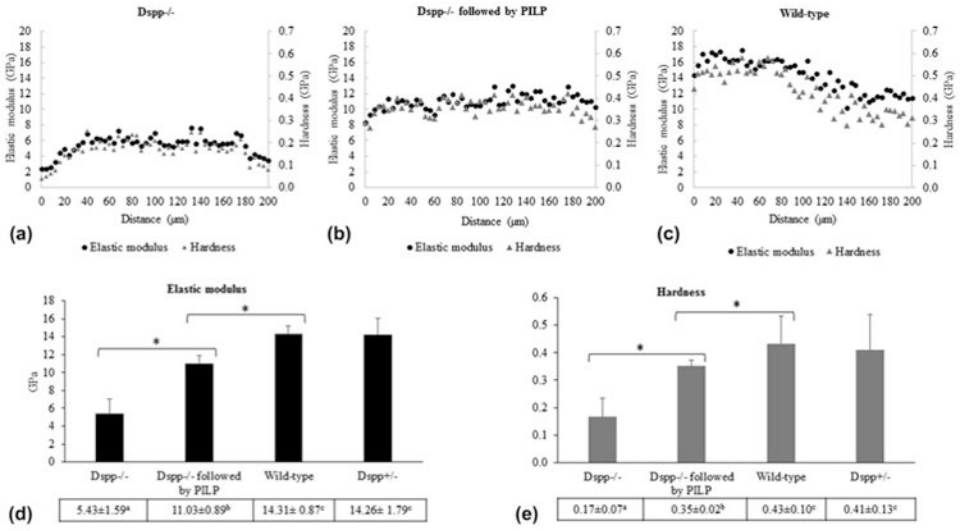

Fig. 1.

Average elastic modulus and hardness values across mouse dentin from mid-coronal to pulp chamber from *Dspp*$^{-/-}$ mice before (A) and after PILP treatments (B) and from wild-type control (C). Total average of elastic modulus (D) and hardness (E) of each group. Means designated with the different superscript letters indicate significant differences between groups, using one-way ANOVA and Tukey's multiple comparison tests (*$P < 0.05$). Mean ± SD.

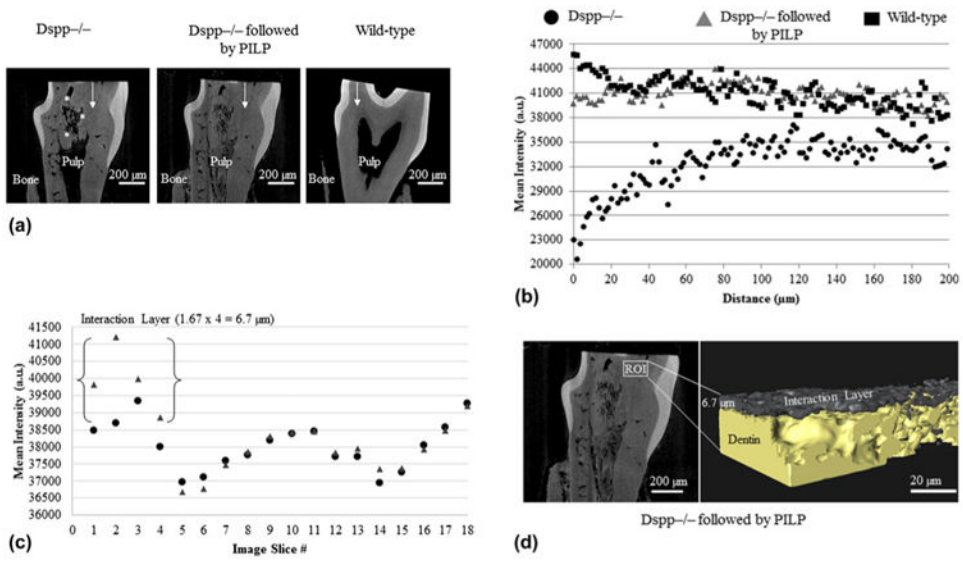

Fig. 2.

(A) X-ray virtual slices illustrating x-ray attenuation data from Micro-XCT tomograms of each specimen. Asterisks identify patchiness at the boundary between mineralized and nonmineralized dentin matrix. (B) Mineral profiles across mouse dentin (white arrow) from mid-coronal to pulp chamber from *Dspp*$^{-/-}$ mice before (round) and after PILP-treatments (triangle) and from wild-type control (rectangle). (C) A mineral intensity profile in arbitrary units (a.u.) illustrating average values from the outer surface through the subsurface layers (through a thickness of about 30 μm) of the *Dspp*$^{-/-}$ dentin before and after PILP-treatments. (D) Image segmentation of *Dspp*$^{-/-}$ mice after PILP-treatments using an Avizo 3D visualization shows a few micrometers interaction layer formed on the dentin surface. Pixel size 5 1.67 μm; Optical magnification = 10× (color online)

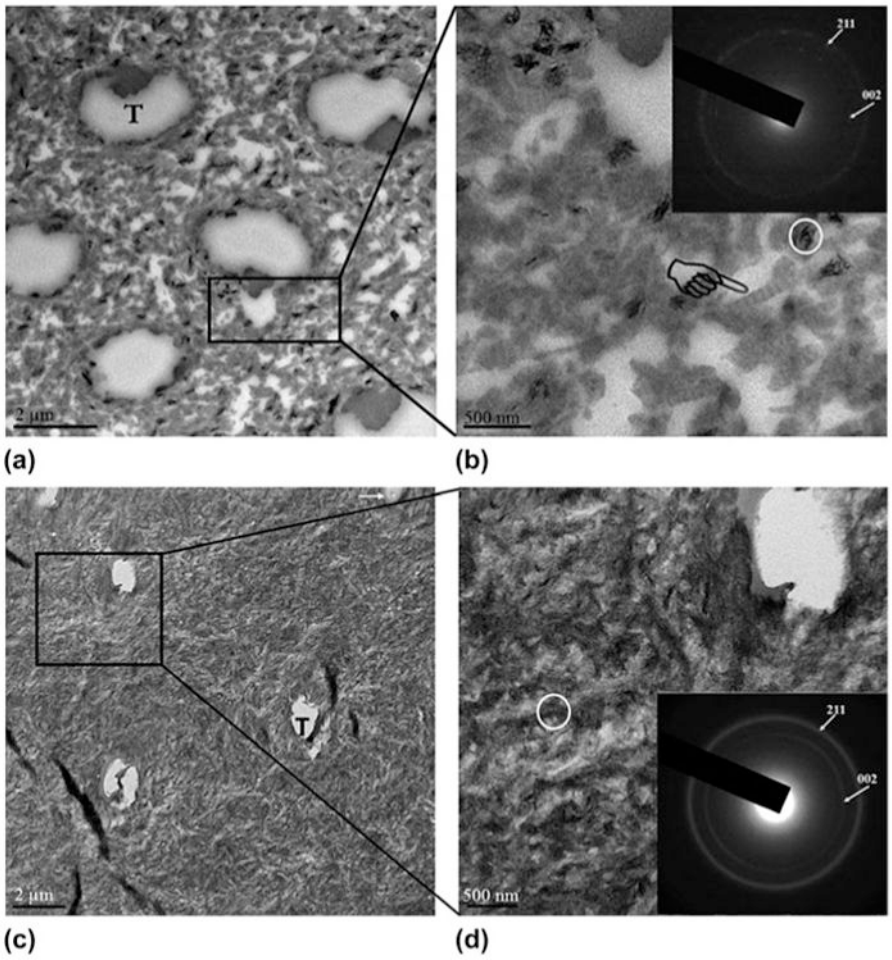

Fig. 3.

TEM images and corresponding SAED patterns of *Dspp*$^{-/-}$ dentin before and after PILP-treatment. The insets in the upper-right corner of (B) and (D) are SAED patterns and are recorded in an area 200 nm in diameter (circle). (A) Before PILP-treatment showing the poorly mineralized patch of collagen matrix. (B) A high-magnification view of (A); these sparsely packed crystals revealed the characteristic type-I collagen D-bands (designated by a pointer). SAED of these sparsely packed crystals revealed the separate diffraction arcs ascribed to the [002] crystal planes, which indicate a preferred orientation of apatite crystals. (C) After PILP-treatment showing electron-dense intrafibrillar and/or extrafibrillar apatite crystals, which were deposited within collagen scaffold. (D) A high-magnification view of (C); the banding pattern of collagen was not visible after mineralization, which is consistent with fibrils containing densely intrafibrillar or extrafibrillar mineral. SAED patterns of this treated dentin revealed continuous ring patterns with indexing confirming the dense of apatite phase. T = dentinal tubules; Arrow = some dentinal tubules were filled with precipitate.